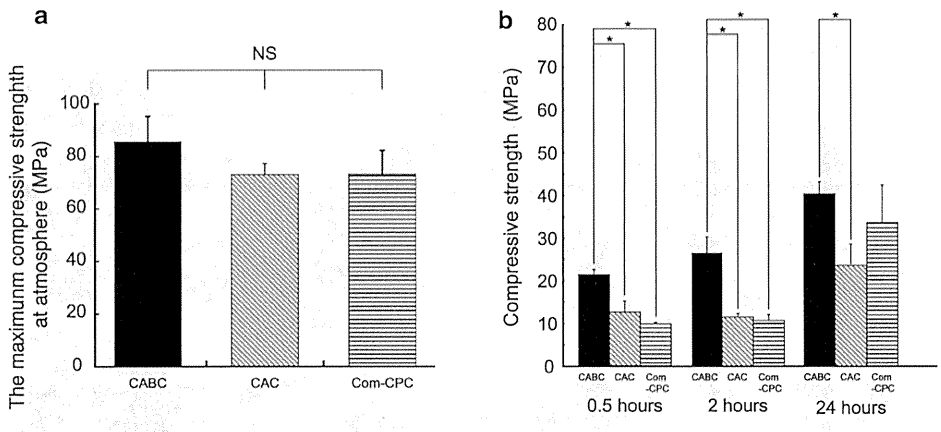

Fig. 6 Compressive strength of CPCs. **a** The maximum compressive strengths of the CPCs after being kept for 5 days. NS means there were no statistically significant differences among these CPCs. **b** Compressive strengths of the CPCs with physiologic saline. Significant differences of $p < 0.05$ are represented by a *single asterisk*

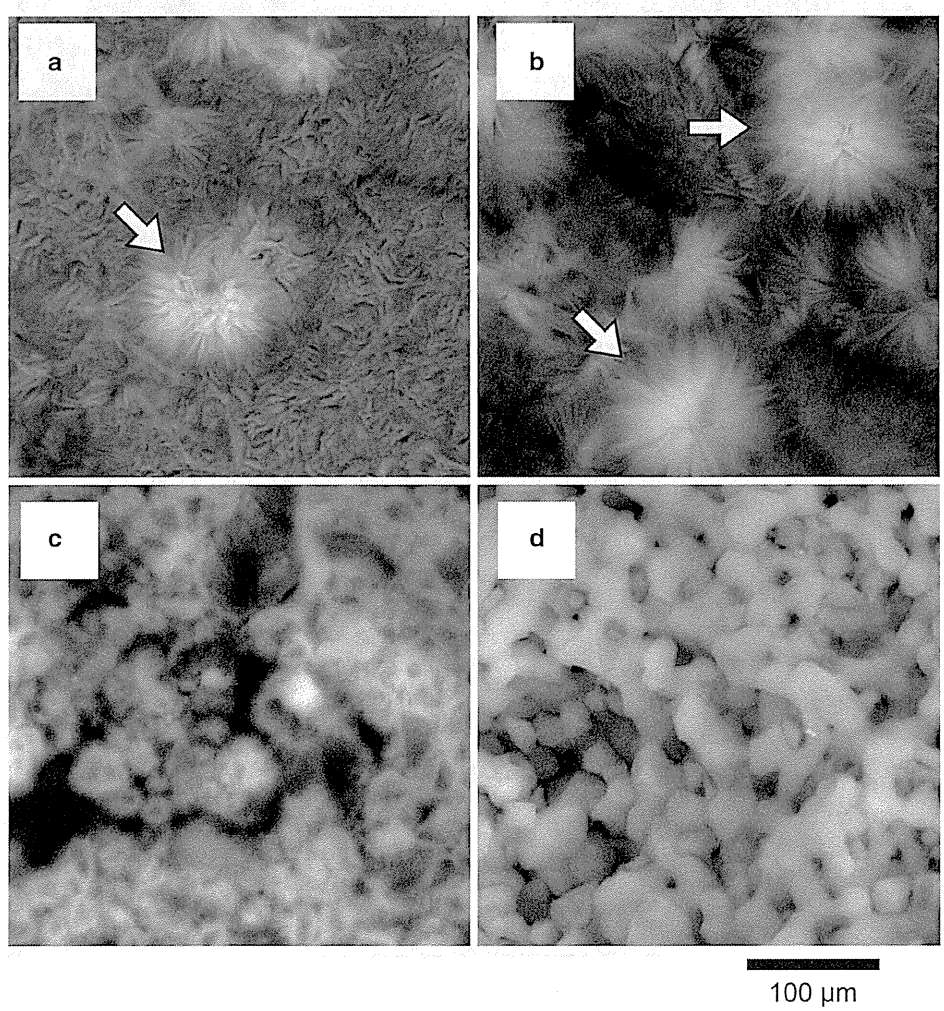

Fig. 7 Apatite-forming ability in SBF after 3 days: **a** CABC, **b** CAC, **c** Com-CPC, and **d** P-CP. *White arrows* indicate apatites

(32 implants from the 4 different implantation periods). At retrieval, no visual signs of inflammatory or adverse tissue reaction were observed.

3.2.1 *Descriptive SEM micrographs and light microscopy after implantation*

3.2.1.1 SEM micrographs Representative SEM images of the samples obtained from the four materials are depicted in Fig. 8. SEM images obtained after each implantation period showed new bone tissue (NB) in contact and attached to these four materials. No fibrous tissue or flesh was observed between the new bone tissue and either of these four materials. The results also revealed that α-TCP granules (white arrows) and/or β-TCP granules (black arrows) had been gradually absorbed into the CABC, CAC, and P-CP samples over time. For the P-CP sample, all of the materials had been completely absorbed after 52 weeks of implantation (Fig. 8p).

3.2.1.2 Histological images of light microscopy Representative histological images recorded by light microscopy from the four materials are shown in Fig. 9. After each implantation period, new bone tissue (red stained) was observed in contact and attached to these four materials (all of the materials were recorded in black). No fibrous tissue or flesh was observed between the new bone tissue and these four materials. For the CABC sample (Figs. 9a, 9b, 9c, and 9d), the CABC was gradually absorbed by the peripheral material over time. Cracks appeared in the CAC

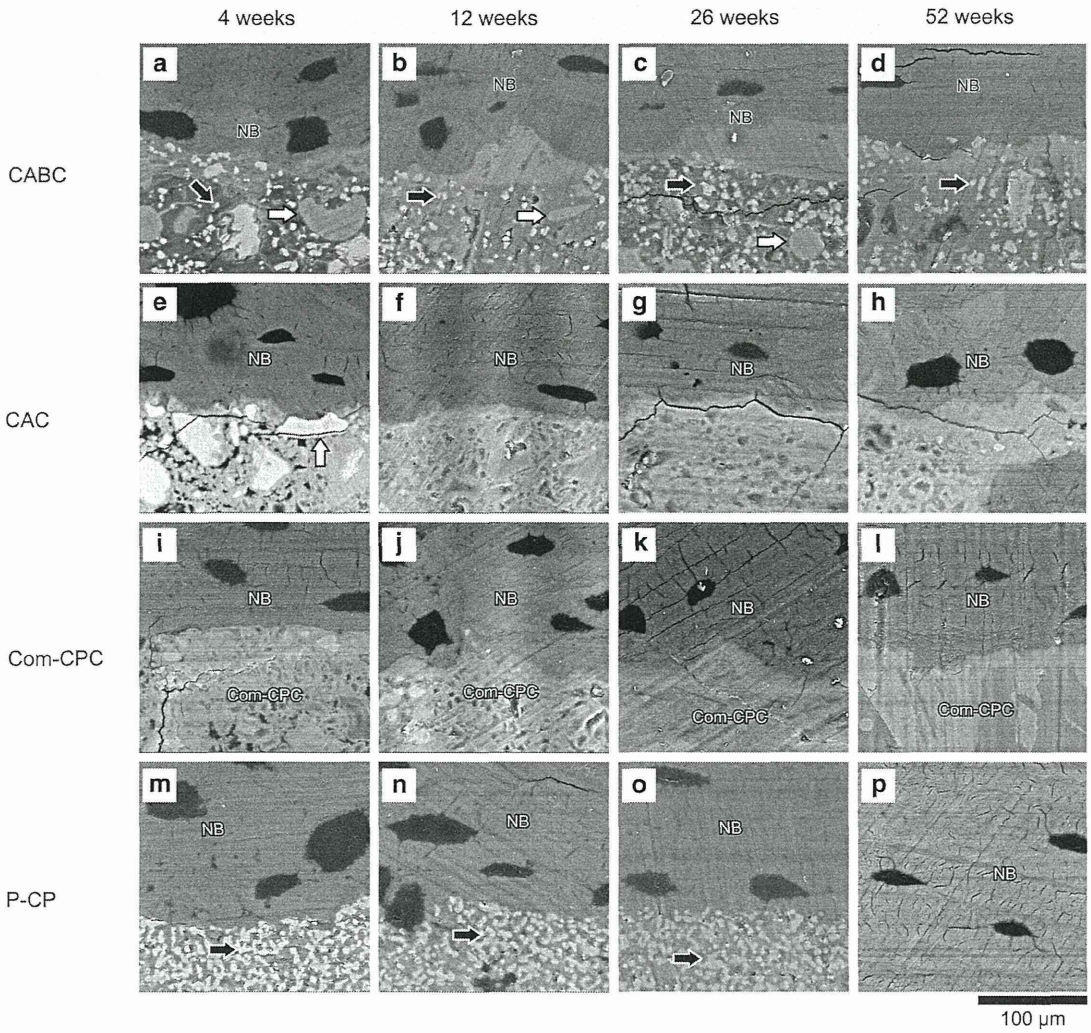

Fig. 8 SEM images of CABC at **a** 4, **b** 12, **c** 26, and **d** 52 weeks of implantation; CAC at **e** 4, **f** 12, **g** 26, and **h** 52 weeks of implantation; Com-CPC at **i** 4, **j** 12, **k** 26, and **l** 52 weeks of implantation; as well as P-CP at **m** 4, **n** 12, **o** 26, and **p** 52 weeks of implantation, respectively. *White arrows* indicate α-TCPs and *black arrows* indicate β-TCPs. NB stands for new bone tissues

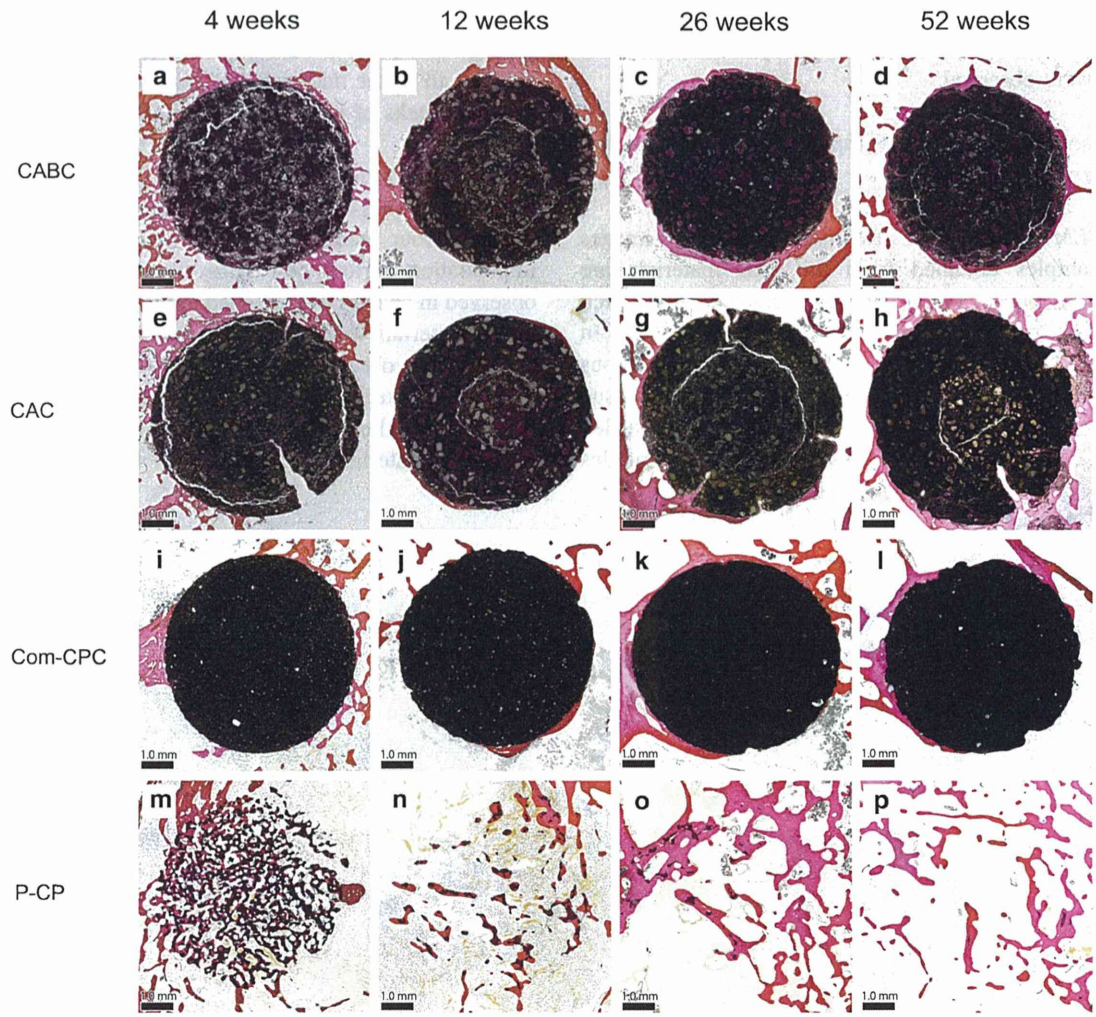

Fig. 9 Histological images of CABC at **a** 4, **b** 12, **c** 26, and **d** 52 weeks of implantation; CAC at **e** 4, **f** 12, **g** 26, and **h** 52 weeks of implantation; Com-CPC at **i** 4, **j** 12, **k** 26, and **l** 52 weeks of implantation; as well as P-CP at **m** 4, **n** 12, **o** 26, and **p** 52 weeks of implantation, respectively (Color figure online)

that were caused by the peripheral material (Figs. 9e, 9g, and 9h). New bone tissue formed around the Com-CPC material (Figs. 9i, 9j, 9k, and 9l), although less bone tissue was observed in this case at each implantation time than was observed around the CABC material, and there was very little absorbed material in Com-CPC.

3.2.2 *Histomorphometry*

3.2.2.1 Bone-material contact index The CABC showed bone-material contact indices of 0.8453 ± 0.17734, 0.8171 ± 0.11766, 0.8139 ± 0.10306, and 0.8546 ± 0.19490 at 4, 12, 26, and 52 weeks of implantation, respectively, whereas CAC gave values of 0.6612 ± 0.15357, 0.5328 ± 0.19065, 0.6375 ± 0.15754, and 0.4926 ± 0.17264 at 4, 12, 26, and 52 weeks of implantation, respectively (Fig. 10a). The corresponding values for Com-CPC were 0.3698 ± 0.32428, 0.5378 ± 0.29172, 0.7214 ± 0.13511, and 0.5256 ± 0.17853, respectively (Fig. 10a). CABC showed statistically significant higher bone-material contact indices than Com-CPC at 4 ($p = 0.00034$), 12 ($p = 0.0067$), and 52 ($p = 0.0000036$) weeks of implantation, and CABC showed statistically significant higher bone-material contact indices than CAC at all time points of implantation ($p = 0.00035$, 0.000030, 0.00050, and 0.0000040 at 4, 12, 26, and 52 weeks, respectively).

3.2.2.2 Material absorbed ratio CABC showed material absorbed ratios of 2.37 ± 1.79, 5.56 ± 4.28, 5.26 ± 2.55 and 6.31 ± 2.74 % at 4, 12, 26 and 52 weeks of implantation, respectively, whereas CAC gave values 2.11 ± 3.05, 4.48 ± 4.30, 3.78 ± 4.53, and 3.08 ± 3.70 % at 4, 12, 26, and 52 weeks of implantation, respectively (Fig. 10b). The corresponding values for Com-CPC were 3.30 ± 1.90, 5.41 ± 2.09, 5.32 ± 2.26, and 4.79 ± 3.36 %, respectively

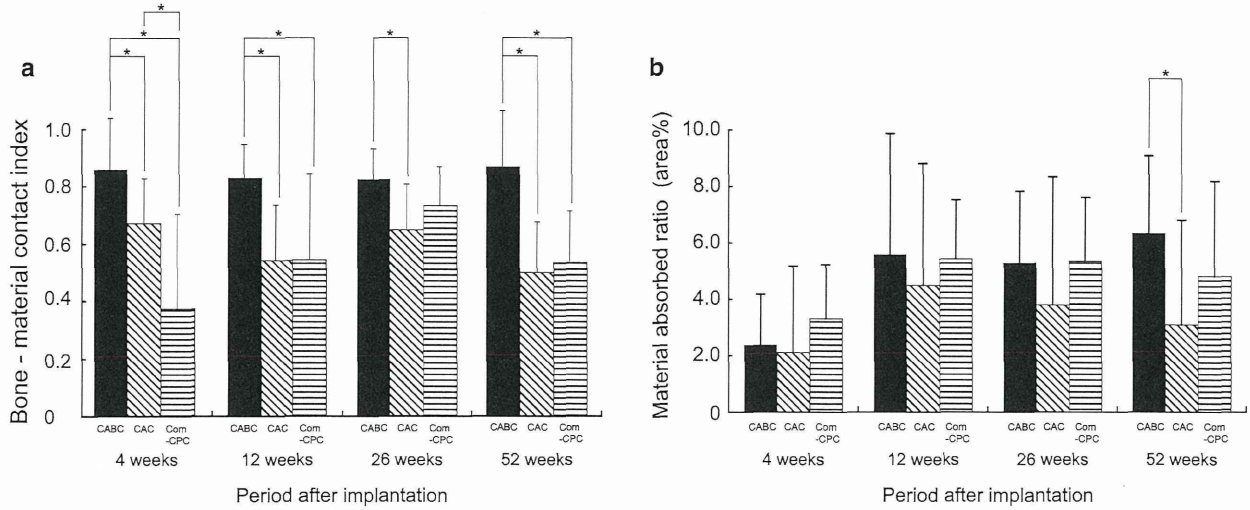

Fig. 10 Quantitative evaluation of bone-material contact index and material absorbed ratio. **a** Bone-material contact index between a CABC, CAC, and Com-CPC after 4, 12, 26, and 52 weeks of implantation. Significant differences of $p < 0.01$ are represented by a *single asterisk*. **b** Material absorbed ratio between CABC, CAC, and Com-CPC after 4, 12, 26, and 52 weeks of implantation. Significant differences of $p < 0.05$ are represented by a *single asterisk*

(Fig. 10b). CABC showed a statistically significant higher material absorbed ratio than CAC at 52 weeks of implantation ($p = 0.029$), but there were no statistically significant differences between CABC and Com-CPC at any of the time points of implantation.

4 Discussion

The setting times observed in the in vitro study of CABC and CAC were statistically significantly shorter than those of Com-CPC at all of the temperatures tested. Analysis by XRD and FT-IR indicated that the citric acid in the CABC and CAC samples had been completely consumed by the formation of calcium chelates with α-TCP and CSP, respectively. The results of these analyses confirmed that CABC and CAC had undergone a hardening process, with chelate bonding occurred between the calcium ions of α-TCP/CSP and the citric acid ions. An equation for chelate bonding between the calcium ions and citric acid ions is shown in Scheme 1. Chelate bonding occurs at faster rate than the hydrolysis of calcium phosphate. The presence of citric acid in the system can therefore improve the workability of the cement paste by greatly increasing the viscosity of the liquid phase [18]. The enhanced compressive strengths of the materials in physiologic saline were attributed to their shorter setting times.

The setting times observed for CABC appeared to be similar to those observed during clinical use. The following handling requirements (in minutes) have been formulated for CPC:

$$3 \leq I < 8$$

$$I - CT \geq 1$$

where CT is the cohesion time, and I is the initial setting time [19, 20].

There is also a requirement for CT to be at least 1 min so that the clinician has at least 1 min to apply and mold the

Scheme 1 Equation for the chelate bonding between the calcium and citric acid ions in CABC and CAC

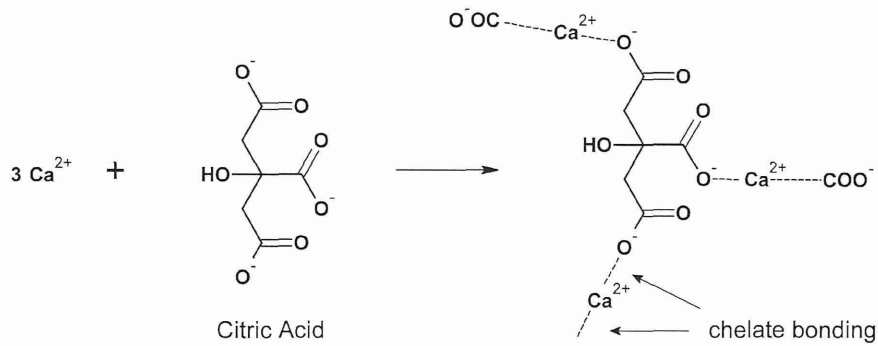

material prior to the beginning of the initial setting time (*I*). For dental applications in clinical practice, *I* must be close to 3 min, whereas orthopedic applications would require the value to be closer to 8 min [18, 21]. For CABC, the *CT* was set at 1 min and *I* was determined to be 5.7 ± 0.3 min at 22 °C. For CAC, the *CT* was set at 1 min and *I* was found to be 11.3 ± 0.6 min at 22 °C. For Com-CPC, the *CT* was set at 1.5 min and *I* was found to be 21.8 ± 0.6 min at 22 °C. These results suggested that CABC was more stable and possessed better handling properties than CAC and Com-CPC immediately after mixing. These results also suggested that the use of CABC would be beneficial in terms of minimizing blood contamination during the setting time.

The maximum compressive strengths of CABC, CAC, and Com-CPC were all around 80 MPa, with no statistically significant differences being observed between the three materials. In contrast, at 0.5 and 2 h in physiologic saline, CABC showed a statistically significantly higher compressive strength than the other materials. Prior to complete hardening of the CABC material, however, granules of β-TCP were worked into the supports to raise the mechanical strength of the cement.

In the current in vivo study, CABC showed a statistically significantly higher bone-material contact index than Com-CPC at 4, 12, and 52 weeks after the implantation process. Furthermore, CABC showed a statistically significantly higher bone-material contact index than CAC at all of the time points measured following the implantation process. The water solubility of CSP, which consists of 41.2 wt% CABC and 50.0 wt% CAC, has been reported to be greater than that of calcium phosphate [22]. Furthermore, CSP is ionized to sodium, calcium, and phosphorous ions in solution, and higher concentrations of calcium and phosphorous ions near to the surface of the material can have a positive influence on its osteoconductivity properties. Consequently, there may have been a high concentration of calcium ions and phosphorous ions near the surfaces of the CABC and CAC materials. Apatite formation can occur in the presence of high concentrations of calcium and phosphorous ions, and this could explain why apatite formed on the surfaces of the CABC and CAC materials after only 1 day in SBF in the current in vitro study, but not on the Com-CPC or P-CP surface (Fig. 7). It was therefore envisaged that CABC and CAC would afford higher levels of osteoconductivity in vivo than Com-CPC. CABC showed a statistically significant higher bone-material contact index than CAC at all of the time points measured after the implantation process. β-TCP alone has been reported to exhibit good osteoconductivity [23], and CABC therefore exhibited higher osteoconductivity in vivo than CAC.

The results of histomorphometry experiments to determine the absorptivity properties of the materials revealed that there were no statistically significant differences between CABC and Com-CPC at any of the time points measured following implantation. In the current study, CABC and Com-CPC showed the same bioresorbability properties. CABC showed a statistically significantly higher absorption ratio than CAC at 52 weeks after the implantation. This higher absorption ratio was attributed to the fact that the β-TCP in the CABC did not participate in the chelate-binding reaction between the calcium ions from the α-TCP/CSP and the citric acid ions. β-TCP is less water soluble than α-TCP or CSP [24], which may have prevented its calcium ions from being available in solution to participate in a chelate-binding reaction. From the histological images of P-CP recorded by SEM (Fig. 8p) and using a light microscope (Fig. 9p), it was clear that the β-TCP, which contained P-CP, had been completely absorbed after 52 weeks of implantation. β-TCP was considered to be more water soluble than the chelate-binding object. These results also provide some indication as to why the CABC showed a statistically significantly higher absorption ratio than CAC, which did not contain β-TCP, at 52 weeks after the implantation. Based on these results, CABC appeared to be a better novel CPC than CAC in terms of its properties.

To date, a wide variety of different bone reinforcing materials have been developed, with the materials themselves being formed from pastes. Products with high post-setting mechanical strength are poorly absorbed and difficult to replace with bone, whereas products that are readily absorbed and replaced with bone have lower post-setting mechanical strength [25–27]. This CABC is characterized by better handling properties, shorter setting time, and higher post-setting mechanical strength in physiologic saline. This material also possesses greater osteoconductivity properties than those of Com-CPC, and therefore represents an attractive alternative bone substitute material for orthopedic or dental use.

5 Conclusions

The results of this preliminary study have shown that our newly developed CPC (CABC: consisting of calcium sodium phosphate, α-TCP, β-TCP, anhydrous citric acid, and glycerol) exhibited a compressive strength of 26.7 ± 3.7 MPa, even after being mixed with physiologic saline, and reached 86.0 ± 9.7 MPa after 5 days with a setting time of 5.7 ± 0.3 min at 22 °C. The second of our newly developed CPCs (CAC: consisting of calcium sodium phosphate, α-TCP, anhydrous citric acid, and glycerol) showed a statistically significantly lower compressive strength than that of CABC in physiologic saline, as well as statistically significantly longer setting times. An

apatite layer formed on the surfaces of the CABC and CAC materials in SBF much earlier than it did in the commercially available CPC (Com-CPC: Biopex®-R). The results of XRD and FT-IR analyses confirmed that the hardening of the CABC and CAC materials involved the formation of a chelate bond between the calcium ions of the α-TCP/CSP and citric acid ions. The results of an animal study confirmed that CABC possessed superior osteoconductivity properties to Com-CPC and equivalent bioresorbability characteristics. Animal studies also confirmed that CABC possessed superior osteoconductivity and bioresorbability properties compared with CAC. Based on these results, CABC clearly satisfies the four essential requirements for a CPC, including good handling properties, short setting time, high post-setting mechanical strength (even with physiologic saline), and high osteoconductivity. CABC therefore represents an attractive alternative bone substitute material.

References

1. Bauer TW, Muschler GF. Bone graft materials. An overview of the basic science. Clin Orthop Relat Res. 2000;371:10–27.
2. Wimmer C, Krismer M, Gluch H, Ogon M, Stockl B. Autogenic versus allogenic bone grafts in anterior lumbar interbody fusion. Clin Orthop Relat Res. 1999;360:122–6.
3. Merkx MA, Maltha JC, Freihofer HP, Kuijpers-Jagtman AM. Incorporation of three types of bone block implants in the facial skeleton. Biomaterials. 1999;20(7):639–45.
4. Sarkar MR, Wachter N, Patka P, Kinzl L. First histological observations on the incorporation of a novel calcium phosphate bone substitute material in human cancellous bone. J Biomed Mater Res. 2001;58(3):329–34.
5. Biddulph SL. Bone donor site. Iliac crest or distal radius? J Hand Surg. 1999;24(6):645–6. doi:10.1054/jhsb.1999.0280.
6. Bohner M, Gbureck U, Barralet JE. Technological issues for the development of more efficient calcium phosphate bone cements: a critical assessment. Biomaterials. 2005;26(33):6423–9. doi:10.1016/j.biomaterials.2005.03.049.
7. Dorozhkin SV. Calcium orthophosphate cements for biomedical application. J Mater Sci. 2008;43(9):3028–57. doi:10.1007/s10853-008-2527-z.
8. Yaszemski MJ, Payne RG, Hayes WC, Langer R, Mikos AG. Evolution of bone transplantation: molecular, cellular and tissue strategies to engineer human bone. Biomaterials. 1996;17(2):175–85.
9. Hollinger JO, Brekke J, Gruskin E, Lee D. Role of bone substitutes. Clin Orthop Relat Res. 1996;324:55–65.
10. Musha Y, Umeda T, Yoshizawa S, Shigemitsu T, Mizutani K, Itatani K. Effects of blood on bone cement made of calcium phosphate: problems and advantages. J Biomed Mater Res. 2010;92(1):95–101. doi:10.1002/jbm.b.31493.
11. Clokie CML, Moghadam H, Jackson MT, Sandor GKB. Closure of Critical Sized Defects With Allogenic and Alloplastic Bone Substitutes. J Craniofacial Surg. 2002;13(1):111–21.
12. Doi Y, Shimizu Y, Moriwaki Y, Aga M, Iwanaga H, Shibutani T, et al. Development of a new calcium phosphate cement that contains sodium calcium phosphate. Biomaterials. 2001;22(8):847–54.
13. Wang X, Chen L, Xiang H, Ye J. Influence of anti-washout agents on the rheological properties and injectability of a calcium phosphate cement. J Biomed Mater Res. 2007;81(2):410–8. doi:10.1002/jbm.b.30678.
14. Knabe C, Berger G, Gildenhaar R, Howlett CR, Markovic B, Zreiqat H. The functional expression of human bone-derived cells grown on rapidly resorbable calcium phosphate ceramics. Biomaterials. 2004;25(2):335–44.
15. Driessens FCM, Boltong MG, Bermudez O, Planell JA. Formulation and setting times of some calcium orthophosphate cements: a pilot study. J Mater Sci–Mater Med. 1993;4(5):503–8. doi:10.1007/BF00120130.
16. Mangram AJ, Horan TC, Pearson ML, Silver LC, Jarvis WR. Guideline for prevention of surgical site infection, 1999. Hospital Infection Control Practices Advisory Committee. Infect Control Hosp Epidemiol. 1999;20(4):250–78.
17. Kokubo T, Kushitani H, Sakka S, Kitsugi T, Yamamuro T. Solutions able to reproduce in vivo surface-structure changes in bioactive glass-ceramic A-W. J Biomed Mater Res. 1990;24(6):721–34. doi:10.1002/jbm.820240607.
18. Dorozhkin SV, Epple M. Biological and medical significance of calcium phosphates. Angew Chem Int Ed Engl. 2002;41(17):3130–46. doi:10.1002/1521-3773.
19. Khairoun I, Boltong MG, Driessens FC, Planell JA. Limited compliance of some apatitic calcium phosphate bone cements with clinical requirements. J Mater Sci–Mater Med. 1998;9(11):667–71.
20. Ginebra MP, Fernández E, Driessens FCM, Boltong MG, Muntasell J, Font J, et al. The effects of temperature on the behaviour of an apatitic calcium phosphate cement. J Mater Sci–Mater Med. 1995;6(12):857–60. doi:10.1007/BF00134332.
21. Driessens FC, Planell JA, Boltong MG, Khairoun I, Ginebra MP. Osteotransductive bone cements. Proc Inst Mech Eng [H]. 1998;212(6):427–35.
22. Jalota S, Bhaduri SB, Tas AC. A new rhenanite (β-$NaCaPO_4$) and hydroxyapatite biphasic biomaterial for skeletal repair. J Biomed Mater Res. 2007;80(2):304–16.
23. Walsh WR, Vizesi F, Michael D, Auld J, Langdown A, Oliver R, et al. β-TCP bone graft substitutes in a bilateral rabbit tibial defect model. Biomaterials. 2008;29(3):266–71.
24. Barralet JE, Tremayne M, Lilley KJ, Gbureck U. Modification of calcium phosphate cement with α-hydroxy acids and their salts. Chem Mater. 2005;17(6):1313–9. doi:10.1021/cm048803z.
25. Kurashina K, Kurita H, Hirano M, Kotani A, Klein CP, de Groot K. In vivo study of calcium phosphate cements: implantation of an alpha-tricalcium phosphate/dicalcium phosphate dibasic/tetracalcium phosphate monoxide cement paste. Biomaterials. 1997;18(7):539–43.
26. Kurashina K, Kurita H, Kotani A, Takeuchi H, Hirano M. In vivo study of a calcium phosphate cement consisting of alpha-tricalcium phosphate/dicalcium phosphate dibasic/tetracalcium phosphate monoxide. Biomaterials. 1997;18(2):147–51.
27. Sarkar MR, Stahl J-P, Wachter N, Schwamborn M, Schnettler RWW, Kinzl L. Defect reconstruction in articular calcaneus fractures with a novel calcium phosphate cement. Eur J Trauma. 2002;28(6):340–8. doi:10.1007/s00068-002-1179-y.

Gait & Posture 40 (2014) 622–627

Contents lists available at ScienceDirect

Gait & Posture

journal homepage: www.elsevier.com/locate/gaitpost

The effect of walking speed on gait kinematics and kinetics after endoprosthetic knee replacement following bone tumor resection

Yusuke Okita [a,*], Noriatsu Tatematsu [b], Koutatsu Nagai [c], Tomitaka Nakayama [d], Takeharu Nakamata [e], Takeshi Okamoto [f], Junya Toguchida [g], Noriaki Ichihashi [a], Shuichi Matsuda [f], Tadao Tsuboyama [a]

[a] Department of Physical Therapy, Human Health Sciences, Graduate School of Medicine, Kyoto University, Kyoto, Japan
[b] Department of Rehabilitation, Kobe Minimally Invasive Cancer Center, Kobe, Japan
[c] Department of Physical Therapy, Hyogo University of Health Sciences, Kobe, Japan
[d] Department of Orthopaedic Surgery, Toyooka Hospital, Toyooka, Hyogo, Japan
[e] Department of Orthopaedic Surgery, Rakuwakai Otowa Hospital, Kyoto, Japan
[f] Department of Orthopaedic Surgery, Kyoto University, Kyoto, Japan
[g] Department of Tissue Regeneration, Institute for Frontier Medical Sciences, Kyoto University, Kyoto, Japan

ARTICLE INFO

Article history:
Received 4 January 2014
Received in revised form 23 June 2014
Accepted 14 July 2014

Keywords:
Bone tumor
Knee endoprosthesis
Walking speed
Gait asymmetry

ABSTRACT

Gait function is one of the most important components of functional outcome evaluation in patients with a tumor around the knee. In addition to walking at a preferred speed, the patients might be sometimes required to walk fast in daily life (e.g., schooling and working) because the major types of bone tumors often occur in adolescence and young adults. Therefore, recovering the ability to walk fast would increase the quality of life of these patients. To clarify which parts of the lower limb are exerted while walking fast, we investigated the kinematic and kinetic changes during fast walking in patients who underwent endoprosthetic knee replacement after bone tumor resection. Laboratory-based gait analysis was performed on eight patients who had undergone endoprosthetic knee replacement following resection of a tumor around the knee. Patients walked at a preferred and faster speed, and the gait parameters were compared between the two walking speeds for each leg. To increase walking speed, patients tended to rely on the bilateral hip, ankle, and contralateral knee to generate additional power. Kinetic analysis showed that involved-side vertical body support was not significantly increased during late stance to increase walking speed, which was associated with a small increase in ankle plantarflexion moment and concentric power. These results suggest to patients after knee reconstruction how to effectively increase their walking speed or redistribute the mechanical load on the muscles and joints to prevent excessive stress on the lower limbs.

1. Introduction

Endoprosthetic knee replacement is often used to preserve joint function in patients with bone tumors around the knee. Recently, surgeons are focusing more on the functional outcomes of patients with musculoskeletal tumors because oncological outcome improves with the help of advanced diagnostic imaging modalities, chemotherapeutic agents, and surgical techniques [1]. Gait function is one of the most important components of functional outcome evaluation in patients who have received treatment for lower extremity tumors. Previous studies have reported that patients had a slower [2,3] or equivalent [4] walking speed compared with healthy subjects, a longer step length of the nonoperated (contralateral) limb than that in the involved limb [5], and decreased foot pressure in the involved limb compared with that in the contralateral limb [6], which can be attributed to insufficient muscle strength and stability of the reconstructed knee.

In previous studies, patients after endoprosthetic replacement were evaluated at a self-selected speed [2–7]. However, increased walking speed is required for some daily life activities that include walking fast to avoid missing the bus or train, crossing at the pedestrian crossing, or walking with other people who walk fast. The major types of bone tumors (osteosarcoma and Ewing's

* Corresponding author. Tel.: +81 75 751 3935; fax: +81 75 751 3948.
E-mail address: okita.yusuke@gmail.com (Y. Okita).

http://dx.doi.org/10.1016/j.gaitpost.2014.07.012
0966-6362/

sarcoma) often occur in adolescents and young adults who may be required to walk faster at school or work. Therefore, recovering the ability to walk fast will increase the quality of life of these patients. This is supported by studies reporting that maximal walking speed reflects a better quality of life in patients with disabilities [8,9].

When walking fast, the mechanical load is increased almost symmetrically in healthy individuals, whereas lower-limb biomechanics are changed asymmetrically in patients after endoprosthetic replacement, possibly because the function of the involved limb is not usually comparable to that of the contralateral limb [10–13]. The gait kinematics (e.g., joint angles) and kinetics (e.g., joint moments and joint powers) of fast walking in these patients are unclear. This study aimed to verify the kinematic and kinetic changes when walking fast in patients who underwent endoprosthetic knee replacement after resection of bone tumors and to help patients effectively learn how to achieve a faster walking speed after knee reconstruction. While walking at a self-selected speed, patients after endoprosthetic knee replacement tend to keep their operated knee extended during stance [4,5,7,13], which inhibits the speed-dependent kinematic and kinetic changes that healthy people exhibit. Therefore, we hypothesized that patients can walk faster by increasing their joint extension moments and powers, not only around the contralateral joints, but also around the involved-side ankle, which can be exerted during walking at a self-selected speed [13] to compensate for the deficiency in the reconstructed knee.

2. Methods

2.1. Study design

In this single-center, cross-sectional study, we included eight patients who underwent endoprosthetic knee replacement after bone tumor resection (mean [range]: age, 30 [19–59] years; height, 1.67 [1.58–1.78] m; weight, 59.9 [45.0–108.5] kg; body mass index, 21.1 [17.6–34.4] kg/m^2) and who could walk without assistive devices at a mean (range) of 91 (12–111) months after primary surgery (Table 1). Of the eight patients, six had an osteosarcoma, one had a giant cell tumor of the bone, and one had a chondrosarcoma. Five patients had a tumor in the distal femur and three in the proximal tibia. Four patients underwent surgical revision: one underwent femoral component replacement alone, one underwent tibial component replacement, and two underwent replacement of all the components. All patients were continuous disease free and could walk without assistive devices. Three types of endoprosthesis were used for reconstruction: the Kyocera Limb Salvage System (KYOCERA Medical Corp., Osaka, Japan) in three patients, the Howmedica Modular Resection System (Stryker Orthopedics, Mahwah, NJ) in three patients, and the JMM K-MAX KNEE System K-5 (KYOCERA Medical Material Corp.) in two patients. The mean (range) bone resection length was 14.4 (12–19) cm and 10.7 (7–13) cm for patients with femoral and tibial tumors, respectively. Measurement was performed at a motion analysis laboratory at the authors' institution. The ethical review board at the authors' institution approved all procedures, and written informed consent was obtained from all the subjects.

2.2. Data collection and processing

Gait analysis was performed using a seven-camera three-dimensional motion analysis system (Vicon MX, Vicon, Oxford, UK) with two force plates (9286A, 60 × 40 cm, Kistler Japan, Tokyo, Japan). All the patients walked along the 6-m walkway at a preferred speed, and a faster speed that was not strictly controlled. A total of 35 retro-reflective markers were attached to body landmarks according to the Plug-in Gait protocol (Vicon). At least five successful trials (defined as foot contact achieved on the various force plates) were collected for each walking speed to ensure reproducibility of the results. Data were collected at a sampling rate of 100 Hz for marker trajectories and 1000 Hz for the force plates.

Marker trajectories were filtered using a Woltring filter [14] with a mean-squared error value of 10. Joint kinematics and kinetics were generated using inverse dynamics analysis within Vicon Nexus software (version 1.7.1, Vicon). Joint moments were filtered by a zero-lag fourth-order Butterworth filter with a cutoff frequency of 6 Hz. Joint powers were calculated by multiplying the joint angular velocities and joint moments on the sagittal plane. Joint moments and powers were normalized to body weight and height. All data were processed using the Vicon Nexus software and MATLAB (2012a, MathWorks, Natick, MA).

2.3. Statistical methods

Walking speeds are presented as mean (SD). The mean ground reaction forces (GRF), joint angles, joint moments, and joint powers were calculated for each walking speed and limb (walking speed: preferred or faster speed; limb: involved or contralateral side). We compared joint kinematic and kinetic parameters between walking speeds (preferred and faster) using the Wilcoxon signed-rank test performed on R (version 2.41.0, R Development Core Team) (Table 2). We also compared the change in each parameter between the two walking speeds for both limbs by using

Table 1
Patient characteristics at the time of measurement.

	Sex/age (y)	Follow-up (mo*)	Diagnosis	Site	Endoprosthesis (hinge type)	Revision	Resected muscles and bone length (cm)	MSTS score (%†)	knee extensor strength‡ (involved/contralateral side) (N m/kg)
1	M/59	47	CS	Tibia	HMRS (rotating)	Yes	None, 13	80	0.3/1.9
2	M/19	51	OS	Femur	JMM-K5 (hingeless)	No	VL (lateral part), 12	80	0.2/1.8
3	M/34	81	GCT	Femur	KLS (fixed)	Yes	None, 12	76.7	0.5/2.5
4	M/24	29	OS	Tibia	HMRS (rotating)	Yes	Soleus (lateral part), 7	86.7	1.1/2.1
5	F/24	34	OS	Femur	KLS (rotating)	No	VI, VM, 13	80	0.2/1.6
6	M/24	12	OS	Femur	KLS (rotating)	Yes	VI, VL, 19	76.6	0.2/1.9
7	M/27	61	OS	Femur	JMM K-5 (hingeless)	No	VI (lateral part), VL, 16	83.3	0.7/3.1
8	M/30	111	OS	Tibia	HMRS (rotating)	No	None, 12	76.7	0.8/3.1

Abbreviations: CS, chondrosarcoma; GCT, giant cell tumor; HMRS, Howmedica Modular Resection System; JMM-K5, Japan Medical Materials K-MAX KNEE System K-5; KLS, Kyocera Limb Salvage System; MSTS, Musculoskeletal Tumor Society; OS, osteosarcoma; VI, vastus intermedius; VL, vastus lateralis; VM, vastus medialis.

* Interval from last surgery (primary or revision).

† Total percentage of the full score.

‡ Peak isokinetic torque measured at 30°/s.

Table 2
The intra- and inter-limb comparisons of gait kinetic and kinematic parameters.

	Involved side				Contralateral side				Inter-limb comparison	
	Preferred	Faster	Speed-dependent change	*P* value (intra-limb)	Preferred	Faster	Speed-dependent change	*P* value (intra-limb)	Difference of speed-dependent change	*P* value (inter-limb)
Ground reaction forces, % BW										
Max. aft force	14.9 (8.9 to 32.7)	22.2 (9.4 to 41.6)	7.2 (0.4 to 13.9)	**0.008**	18.3 (15.2 to 23.8)	30.1 (19.1 to 32.8)	10.3 (1.9 to 15.9)	**0.008**	4.9 (−7.0 to 7.4)	0.19
Max. fore force	19.7 (10.5 to 21.7)	23.2 (11.5 to 30.9)	5.0 (1.0 to 9.3)	**0.008**	24.6 (19.3 to 31.1)	31.9 (27.8 to 37.0)	7.3 (4.2 to 11.4)	**0.008**	3.5 (−1.9 to 4.3)	**0.04**
Max. vertical force (1st)	100.5 (90.3 to 108.6)	114.6 (92.5 to 138.4)	16.2(−1.5 to 29.8)	**0.016**	111.6 (101.9 to 118.4)	134.9 (118.5 to 151.1)	23.3 (16.7 to 40.7)	**0.008**	12.7 (−11.1 to 30.7)	0.11
Max. vertical force (2nd)	102.0 (96.9 to 107.6)	99.0 (93.4 to 117.7)	−1.6 (−7.7 to 10.1)	0.74	115.9 (111.0 to 123.6)	125.6 (120.0 to 139.2)	11.7 (−0.6 to 17.6)	**0.016**	7.5 (6.2 to 16.6)	**0.008**
Joint angles (°)										
Max. stance hip flexion	33.9 (22.1 to 40.5)	38.5 (26.1 to 40.9)	3.7 (0.3 to 5.3)	**0.008**	40.4 (24.1 to 45.0)	45.1 (27.1 to 49.0)	5.2 (2.7 to 8.7)	**0.008**	2.0 (−1.0 to 6.0)	**0.02**
Max. hip extension	10.2 (−3.4 to 19.2)	11.7 (−6.6 to 21.4)	1.4 (−3.2 to 3.2)	0.31	9.8 (−3.5 to 22.8)	13.4 (−3.3 to 28.4)	3.1 (0.1 to 6.1)	**0.006**	2.1 (0.6 to 3.4)	**0.008**
Max. swing hip extension	37.0 (24.9 to 51.0)	40.8 (27.0 to 54.0)	2.5 (−4.0 to 5.4)	0.08	40.2 (25.4 to 46.0)	43.5 (25.9 to 48.3)	3.3 (0.5 to 6.5)	**0.008**	0.1 (−1.5 to 6.3)	0.55
Knee flexion at contact	4.7 (−3.4 to 11.6)	5.5 (−6.4 to 11.9)	0.3 (−3.0 to 2.7)	0.55	8.2 (4.4 to 15.6)	11.3 (3.7 to 17.9)	2.7 (−2.9 to 5.8)	0.08	2.8 (−4.9 to 6.1)	0.20
Max. stance knee flexion	10.3 (−3.2 to 17.6)	10.0 (−5.4 to 27.9)	0.7 (−2.2 to 10.3)	0.25	24.2 (20.5 to 29.4)	31.7 (26.1 to 36.8)	6.4 (2.4 to 13.2)	**0.008**	3.8 (−5.3 to 12.3)	0.08
Max. swing knee flexion	65.5 (36.5 to 75.6)	68.0 (43.5 to 82.2)	5.0 (1.5 to 7.0)	**0.008**	65.9 (58.7 to 71.4)	67.3 (61.7 to 73.6)	3.3 (−5.2 to 6.1)	0.07	−2.2 (−6.7 to 2.4)	0.11
Dorsiflexion at contact	−0.9 (−12.4 to 8.2)	−0.7 (−13.5 to 8.5)	−0.5 (−2.3 to 1.9)	0.55	0.8 (−2.2 to 7.6)	2.8 (−2.4 to 9.6)	1.2 (−1.2 to 2.8)	0.15	1.6 (−1.3 to 3.2)	0.04
Max. stance plantarflexion	11.2 (3.7 to 18.7)	12.1 (2.1 to 17.5)	−0.6 (−1.6 to 2.3)	0.55	2.9 (−1.0 to 7.0)	2.7 (−2.9 to 7.4)	−1.1 (−3.8 to 1.9)	0.15	−1.7 (−2.6 to 3.2)	0.46
Max. stance dorsiflexion	11.9 (9.5 to 20.3)	11.4 (8.6 to 20.8)	−1.0 (−2.6 to 0.5)	0.08	15.8 (9.5 to 23.3)	13.6 (8.9 to 21.5)	−2.2 (−3.9 to 0.0)	**0.016**	−0.9 (−3.0 to 0.8)	0.11
Joint moments (Nm/(kg m))										
Max. stance hip extension moment	0.264 (0.151 to 0.441)	0.461 (0.214 to 0.505)	0.113 (0.050 to 0.242)	**0.008**	0.328 (0.151 to 0.828)	0.391 (0.236 to 1.006)	0.102 (−0.036 to 0.178)	**0.02**	−0.095 (−0.152 to 0.128)	0.46
Max. stance hip flexion moment	0.525 (0.247 to 0.741)	0.648 (0.283 to 1.033)	0.110 (0.002 to 0.293)	**0.008**	0.609 (0.371 to 0.711)	0.757 (0.504 to 1.001)	0.141 (0.086 to 0.299)	**0.008**	0.033 (0.007 to 0.084)	**0.008**
Max. early-stance knee extension moment	0.140 (0.035 to 0.262)	0.169 (−0.037 to 0.385)	0.028 (−0.072 to 0.123)	0.25	0.433 (0.100 to 0.619)	0.662 (0.132 to 0.943)	0.277 (0.032 to 0.337)	**0.008**	0.203 (0.022 to 0.409)	**0.008**
Max. stance dorsiflexion moment	0.056 (0.024 to 0.207)	0.059 (0.015 to 0.249)	0.011 (−0.015 to 0.086)	0.25	0.066 (−0.005 to 0.136)	0.080 (−0.008 to 0.141)	0.006 (−0.012 to 0.030)	0.11	−0.001 (−0.099 to 0.021)	0.84
Max. plantarflexion moment	0.668 (0.641 to 0.811)	0.672 (0.605 to 0.921)	0.007 (−0.037 to 0.110)	0.46	0.890 (0.766 to 1.009)	0.991 (0.858 to 1.142)	0.093 (−0.028 to 0.191)	**.016**	0.076 (−0.032 to 0.184)	**0.02**
Joint powers (W/(kg m))										
Max. early−stance hip power	0.365 (0.141 to 0.732)	0.682 (0.265 to 1.076)	0.265 (0.103 to 0.488)	**0.008**	0.325 (0.077 to 1.773)	0.578 (0.155 to 2.471)	0.266 (−0.061 to 0.698)	0.04	−0.142 (−0.376 to 0.595)	0.74
Min. late-stance hip power	−0.570 (−1.198 to−0.413)	−1.067 (−1.510 to −0.433)	−0.356 (−0.918 to −0.020)	**0.008**	−0.636 (−0.790 to −0.336)	−1.087 (−1.625 to −0.493)	−0.451 (−0.963 to −0.140)	**0.008**	−0.040 (−0.377 to 0.235)	0.64
Min. early-stance knee power	−0.033 (−0.212 to −0.000)	−0.076 (−0.569 to 0.000)	−0.041 (−0.357 to 0.025)	0.04	−0.517 (−0.890 to −0.116)	−1.439 (−2.193 to −0.038)	−0.883 (−1.534 to 0.077)	**0.016**	−0.690 (−1.477 to −0.077)	**0.016**
Max. early-stance knee power	0.109 (0.014 to 0.215)	0.144 (0.043 to 0.643)	0.052 (−0.070 to 0.520)	0.54	0.506 (0.344 to 0.706)	1.099 (0.734 to 1.796)	0.715 (0.296 to 1.089)	**0.008**	0.392 (0.203 to 1.064)	**0.008**
Min. ankle power	−0.547 (−0.739 to −0.435)	−0.660 (−1.066 to −0.483)	−0.133 (−0.390 to 0.055)	**0.016**	−0.469 (−0.816 to −0.359)	−0.344 (−0.868 to −0.243)	0.091 (−0.222 to 0.304)	0.46	0.224 (−0.087 to 0.487)	**0.02**
Max. ankle power	2.460 (1.159 to 3.215)	3.257 (1.459 to 6.098)	0.723 (−0.054 to 2.882)	0.016	3.128 (1.694 to 4.264)	4.263 (2.421 to 7.431)	1.245 (0.247 to 3.809)	**0.008**	0.405 (−0.203 to 1.160)	**0.02**

Student's paired *t*-test with Holm correction (statistically significant values in bold).
Abbreviations: Max., maximum; Min., minimum.

the Wilcoxon signed-rank test to assess inter-limb difference. Statistical significance was adjusted using Holm's correction for multiple comparisons because we compared each variable three times (intra-limb [involved and contralateral side] and an inter-limb comparisons). All graphics were generated by R.

3. Results

3.1. Spatiotemporal gait parameters

The preferred walking speed was 1.21 (0.14) m/s, whereas the faster walking speed was 1.62 (0.22) m/s. Cadence was 110.6 (4.4) step/min at the preferred speed and 128 (9.1) step/min at the faster speed. Stride length was greater during the faster walking speed than during the preferred walking speed for both limbs (involved limb: preferred 1.31 [0.14] m, faster 1.52 [0.16]; contralateral limb: preferred 1.31 [0.14] m, faster 1.53 [0.19] m).

3.2. Ground reaction forces

The first and second peak of the fore-aft GRF and the first peak of the vertical GRF were significantly greater during the faster walking speed for both limbs, whereas the second peak of the vertical GRF significantly increased only for the contralateral limb (Fig. 1, Table 2). The greatest difference in the peak GRFs was observed in the contralateral first peak of vertical GRF (23.3%BW, Table 2). The inter-limb comparison showed a greater change in the contralateral aft and vertical forces during late stance compared with those of the involved side (Table 2).

3.3. Joint kinematics

Hip flexion angles at initial contact were greater at the faster speed for both limbs, whereas the maximal hip extension angle during stance and the maximal hip flexion angle during swing were significantly greater only for the contralateral limb (Fig. 2, Table 2). Maximal knee flexion angles during early stance were significantly greater only for the contralateral side, and those during swing were significantly greater only for the involved side. Maximal dorsiflexion angles during stance were significantly increased at the faster walking speed only on the contralateral side. The inter-limb comparison showed a greater change in the contralateral stance hip flexion and extension compared with those of the involved side (Table 2).

3.4. Joint moments

Maximal hip flexion and extension moments were significantly greater at the faster walking speed for both limbs. Maximal knee extension moment during early stance and maximal ankle plantarflexion moment were significantly increased at the faster walking speed only on the contralateral side (Fig. 2, Table 2). The inter-limb comparison showed greater speed-dependent changes in the maximal hip and knee extension moment, and maximal ankle plantarflexion moment for the contralateral side (Table 2)

3.5. Joint powers

Maximal positive (concentric) hip power during early stance and maximal negative (eccentric) ankle power were significantly increased at the faster walking speed only on the involved side, whereas a significant increase in the maximal and minimal knee joint power and maximal ankle concentric power was found only for the contralateral side. The inter-limb comparison showed significant differences in the changes of the knee and ankle powers (Table 2).

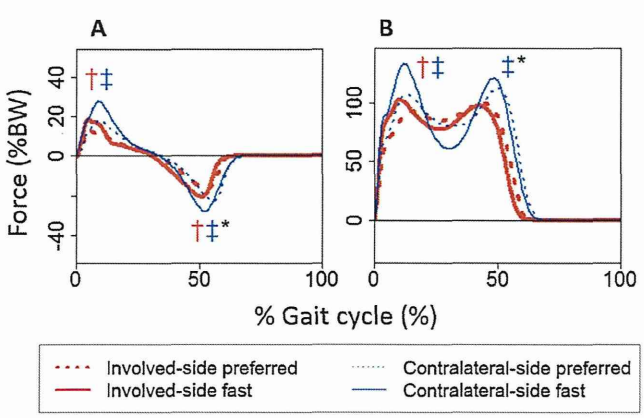

Fig. 1. Ground reaction forces. The dashed lines represent mean values for the preferred walking speed. The solid lines represent the mean values for the faster walking speed. The thick lines are for the involved side. (A) fore-aft; (B) vertical. † Statistically significant for the intra-limb comparison in the involved side, and ‡ in the contralateral side. * Statistically significant for the inter-limb comparison.

4. Discussion

Walking faster in healthy people is usually assumed to induce a symmetric change in gait biomechanics, suggesting that an increased musculoskeletal load is distributed almost equally to both legs. In this study, we found several asymmetric changes in gait kinematics and kinetics in patients who underwent endoprosthetic knee replacement after bone tumor resection. This asymmetry indicates that the gait pattern is adapted to protect the reconstructed knee joint from excessive stress or to avoid using the involved-side quadriceps muscles when the musculoskeletal load increases as the patients walk faster.

For healthy subjects, all the four peaks of fore-aft and vertical GRF increased with faster walking [15]. Previous kinematic studies have shown that faster walking is related to increased hip flexion and extension angles [15,16], hip flexion–extension range [17], knee flexion during stance [17–19] and swing [15–17,19], and decreased maximal ankle dorsiflexion [16,18]. For joint moments, the relationships between walking speed and increased maximal hip flexion and extension moment [15,16,20]; knee flexion moment during stance [15], swing [20], and at a maximum [16]; stance knee extension moment [15,19,20]; and maximal ankle dorsiflexion and plantarflexion moment [16] have been reported. For joint powers, walking speed can be related to the maximal stance hip concentric and eccentric power [15,16,20], knee concentric and eccentric power [15,16,20,21], and maximal ankle concentric power [15,16,20,21]. Nonlinear relationships with walking speed have been observed in some parameters (e.g., maximal ankle plantarflexion moment [20]) whereas others have linearity (e.g., hip flexion angle at foot contact [15]).

Among the four peak values of the GRF, only the second peak of the involved-side vertical GRF did not significantly change at a faster walking speed, whereas previous studies have reported that all of the four peak values tended to increase in healthy subjects during faster walking [15]. These results suggest that increasing body support on the involved limb during late stance is not an efficient strategy at faster walking speeds in patients who underwent endoprosthetic knee replacement, possibly because it might also cause an increased mechanical load on the endoprosthetic knee. Dysfunction of the involved-side calf muscles might be another factor for this observed small change in the involved-side body support during late stance. Detachment of the gastrocnemius that is required for distal femur resection or the surgical invasion of calf muscles that is required for a proximal tibial resection might explain this involved-side finding. The significant increase in the contralateral vertical GRF during early stance might compensate for the involved-side vertical GRF at push-off in the double supporting phase when walking faster. The contralateral vasti and gluteus maximus muscles that are involved in body support during early stance [22] might have an important role in walking faster, particularly in this population. The inter-limb comparison showed that the contralateral side exhibited a significantly greater increase in the second peak of the aft and vertical GRF, which suggests that the contralateral plantarflexors which provide body support and propulsion [22,23], also greatly contribute to faster walking.

Kinematic and kinetic analysis showed an asymmetric change in the hip, knee, and ankle gait parameters. The small change in the involved-side hip extension observed at a faster walking speed might be associated with the small observed change in the involved-side second peak of vertical GRF, maximal ankle plantarflexion moment, and maximal ankle concentric power, all of which work for push-off. Asymmetry in the knee kinematics